Atypical language network lateralization is reflected throughout the macroscale functional organization of cortex

Loïc Labache[a,*], *Tian Ge*[b, c, d], *B.T. Thomas Yeo*[e, f, g, h, i], *Avram J. Holmes*[a, j, k]

Hemispheric specialization is a fundamental feature of human brain organization. However, it is not yet clear to what extent the lateralization of specific cognitive processes may be evident throughout the broad functional architecture of cortex. While the majority of people exhibit left-hemispheric language dominance, a substantial minority of the population shows reverse lateralization. Using twin and family data from the Human Connectome Project, we provide evidence that atypical language dominance is associated with global shifts in cortical organization. Individuals with atypical language organization exhibited corresponding hemispheric differences in the macroscale functional gradients that situate discrete large-scale networks along a continuous spectrum, extending from unimodal through association territories. Analyses revealed that both language lateralization and gradient asymmetries are, in part, driven by genetic factors. These findings pave the way for a deeper understanding of the origins and relationships linking population-level variability in hemispheric specialization and global properties of cortical organization.

A primary architectural feature of the human brain is its homotopy, with each hemisphere exhibiting broadly comparable spatial organization in terms of cytoarchitecture, macroscopic anatomy, and associated large-scale functional systems[1–5]. Despite this fundamentally symmetrical plan, common to the vast clade of animals known as the bilateria[6], the presence of functional asymmetries have been a leading principle of human evolution[7] and, more broadly, the organization of the metazoan nervous system[6]. The hemispheric specialization of a range of specific functions has been well characterized, with one of the most widely investigated being a left-lateralized high-order language network that encompasses aspects of the anterior and posterior cortices[8]. However, while the lateralization of brain functions and associated behaviors has fascinated neuroscientists for over a century[9,10], the origins, mechanisms, and consequences of hemispheric specialization are still largely unknown[11–14]. In this regard, the extent to which the asymmetrical organization of discrete processes may be evident throughout the macroscale functional organization of the cortical sheet remains an open question[15].

The detailed anatomical study of the brain systems supporting language began through the post-mortem examination of patients with acquired brain injuries and aphasias. These seminal studies revealed a set of interconnected regions in the anterior and posterior cortices of the left hemisphere that underpin healthy language functioning[16], including Broca's area within the inferior frontal gyrus adjacent to the somato/motor network and Wernicke's area within the posterior superior temporal cortex. The presence of this left lateralized system has been supported by converging evidence from *in vivo* imaging studies of language function in healthy populations[17] and, more recently, data-driven algorithms that parcelate cortex into discrete functional networks across a variety of task contexts[8,18]. Critically however, the left-hemispheric dominance of the language system is not fixed across development or ubiquitous in the general populations, where atypical organization has been observed[19–21]. Although some anatomical and functional hemispheric asymmetries appear early in human development[22], language is distributed symmetrically in children, with lesions to either hemisphere resulting in an equal likelihood of associated deficits[23]. From early to late adolescence, there is a gradual transition to left-hemisphere dominance in the ma-

[a] Department of Psychology, Yale University, New Haven, US-CT 06520. [b] Psychiatric and Neurodevelopmental Genetics Unit, Center for Genomic Medicine, Massachusetts General Hospital, Boston, US-MA 02114. [c] Center for Precision Psychiatry, Department of Psychiatry, Massachusetts General Hospital, Boston, US-MA 02114. [d] Stanley Center for Psychiatric Research, Broad Institute, Cambridge, US-MA 02142. [e] Department of Electrical and Computer Engineering, Centre for Sleep and Cognition, National University of Singapore, Singapore, SG 119077. [f] Department of Electrical and Computer Engineering, Centre for Translational Magnetic Resonance Research, National University of Singapore, Singapore, SG 119077. [g] N.1 Institute for Health, National University of Singapore, Singapore, SG 119077. [h] Martinos Center for Biomedical Imaging, Massachusetts General Hospital, Charlestown, US-MA 02129. [i] National University of Singapore Graduate School for Integrative Sciences and Engineering, National University of Singapore, Singapore, SG 119077. [j] Department of Psychiatry, Yale University, New Haven, US-CT 06520. [k] Wu Tsai Institute, Yale University, New Haven, US-CT 06520. *e-mail: loic.labache@yale.edu

jority of the population[14], with atypical language organization evident in ~10 percent of individuals[24,25]. This flipped profile of a right hemisphere language system is more likely to be observed in left-handed individuals[26], although not specific to this group. In right-handed adults, 2% to 8% show a dominance reversal[27]. However, the exact mechanisms of brain lateralization are still largely unknown, as are the associated consequences on broader properties of brain organization.

The cerebral cortex is comprised of a dense tapestry of areal units embedded in corresponding processing streams and housed within associated large-scale functional networks[28,29]. The topographic organization of this complex interdigitated network architecture is evident in the presence of functional gradients that situate discrete networks along continuous spectra[30]. The spatial arrangement of areal parcels along these global gradients, for instance along a principal gradient anchored on one end by the unimodal (somatosensory/motor and visual) regions and the other by the cortical association areas that underpin complex cognition[31], reflect a fundamental property of brain organization[32,33]. Converging evidence for these macroscale gradients has been established through *in vivo* imaging measures of function, anatomy[34], and areal allometric scaling[35], as well as histology-derived assessments of cytoarchitecture[36,37] and cortical gene transcription[38–40] (for review see[32]). Intriguingly, there is a strong correspondence between the relative positions of parcels along these gradients and the extent to which they share common cortical microstructure, connectivity, and profiles of gene expression, while recent work suggests that the organization of cortical gradients differs between the two hemispheres[41,42]. Building upon these discoveries, a core goal of the present work is to characterize the organization and lateralization of the language network in relation to the mosaic of functionally distinct large-scale networks and associated macroscale connectivity gradients that span the cortical sheet.

Here, using a recently developed higher-order language atlas[8], we worked to determine the extent to which typical and atypical language lateralization is reflected across the functional architecture of the cerebral cortex. First, through a combination of resting-state functional MRI (fMRI) and task activation studies of language, we establish the presence of typical (92% of sample) and atypical (8% of sample) individuals within the Human Connectome Project (HCP) database[43]. Second, we provide evidence that atypical language lateralization is associated with global shifts in cortical organization. To do so, we applied the dimensionality reduction approach of diffusion map embedding[30] to resting-state data to extract a global framework that accounts for the dominant connectome-level connectivity patterns within each hemisphere. Individuals with atypical language organization exhibited corresponding hemispheric differences in the macroscale functional gradients. This pattern was preferential to functional networks within association cortex. Third, twin-based heritability analyses revealed that both language lateralization and gradient asymmetries are, in part, driven by genetic factors. In doing so, our analyses reveal evidence linking the lateralization of language with broad changes in the functional organization of the cortical sheet.

Results

Identification of Atypically Lateralized Individuals for Language. We investigated the functional connectivity architecture of typically and atypically lateralized language functions in human cortex using task and resting-state fMRI data acquired at 3T (*n*=995, 110 left-handers) as a part of the Human Connectome Project[43]. Demographics are available in the *Methods* section (HCP participants). Language lateralization of each participant was assessed using SENSAAS, a higher-order language atlas[8]. In brief, two task-induced functional asymmetries during a language task[44] were obtained. First, at the network level, averaging across associated parcels, and second, within language network hubs, corresponding to Broca's and Wernicke's areas[8]. Three resting-state variables were also used to assess language lateralization. Two of which characterized the intra-hemispheric organization of the language network at rest, operationalized as the sum and the asymmetry of the average language network functional connectivity strength. The last metric characterized the homotopic inter-hemispheric connectivity of the language network. Taken together, these 5 functional metrics revealed the organization of the higher-order language network (Fig. 1A). The study sample was divided into groups based on their intra- and inter-hemispheric language network organization derived through an agglomerative hierarchical clustering procedure as described by Labache and colleagues[25].

Hierarchical classification established the presence of 3 groups: a strong typical group characterized by a strong leftward asymmetry during language task performance, a mild typical group with moderate leftward asymmetry, and atypical individuals showing a rightward asymmetry (Fig. 1B), reflecting ~8 percent of the study population. The associated group demographics are available in Supplementary Table 1.

We next examined the extent to which language lateralization was reflected across each of the 5 features used to derive the higher-order language network (Fig. 1C). Analysis of covariance allowed us to replicate previous results conducted on an in-

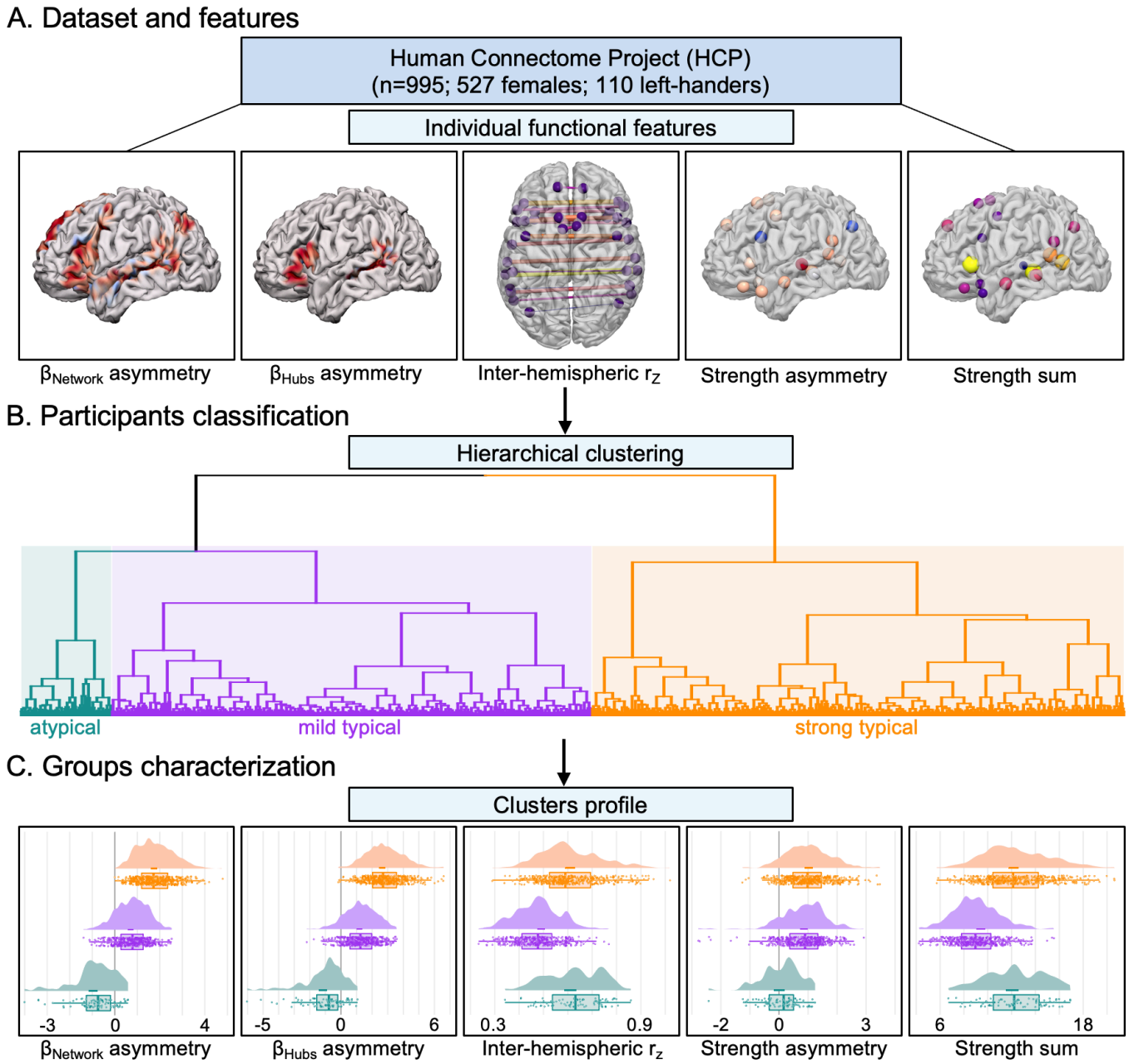

Fig. 1 | Identification and characterization of language lateralization in 995 HCP participants. Overview of preprocessing workflow. **(A)** The five individual functional metrics used to derive the sentence-processing supramodal network[25]. The average BOLD asymmetries values in the story-math contrast both at the network level ($\beta_{Network}$ asymmetry) and hubs level (β_{Hubs} asymmetry), the average homotopic inter-hemispheric intrinsic correlation at the network level (inter-hemispheric r_z), and both the asymmetry (strength asymmetry) and the sum (strength sum) of the average strength at the network level. **(B)** Hierarchical clustering resulted in the identification of three populations with varying degrees of language organization. Consistent with prior work[25], the first cluster with strong leftward asymmetries was named strong typical (n=480, 36 left-handers, orange in the dendrogram), the second cluster exhibiting moderate leftward asymmetry was labeled mild typical (n=433, 48 left-handers, purple in the dendrogram), and the third with strong rightward asymmetries was named atypical (n=82, 26 left-handers, blue in the dendrogram). **(C)** Raincloud plots display the five functional metrics within each identified group. r_z, Fisher z-transformation correlation.

dependent sample of 287 healthy volunteers from the BIL&GIN database[45]. Here, follow-up analyses were conducted to confirm that a single functional metric did not solely drive the results. Language lateralization was evident across each of the 5 functional language features included in the hierarchical classification (see Supplementary Table 2-6). Task-induced functional asymmetries confirmed the rightward lateralization of atypical individuals both at the network (μ=-0.96±0.18) and hubs level (μ=-1.16±0.26, both ps<10^{-4}), as well as a more leftward lateralized language network in strong ($\mu_{network}$=1.74±0.14 $p_{network}<10^{-4}$, μ_{hubs}=2.64±0.19 $p_{hubs}<10^{-4}$) than in mild typical participants ($\mu_{network}$=0.70±0.12 $p_{network}<10^{-4}$, μ_{hubs}=1.17±0.17 $p_{hubs}<10^{-4}$) both at the network and hub level. Intrinsic functional connectivity strength asymmetry profiles revealed that atypical individuals possess

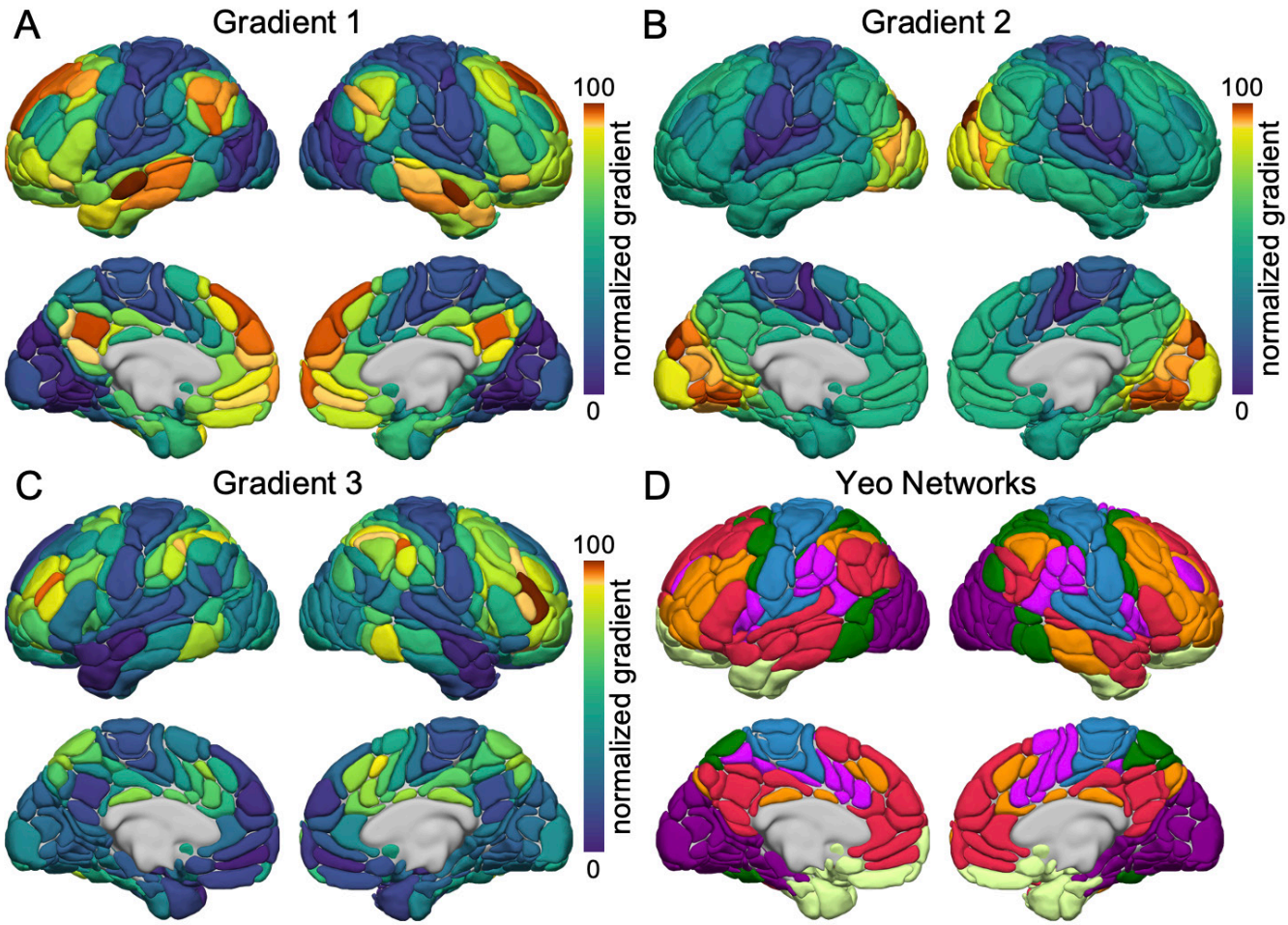

Fig. 2 | The dominant gradients of functional connectivity across the cortical sheet. The first three components resulting from diffusion embedding of the functional connectome connectivity matrix (as defined by Margulies and colleagues[30], dimension reduction technique = diffusion embedding, kernel = normalized angle, sparsity = 0.9). **(A)** The principal gradient of connectivity transitioning from the unimodal (blue) to the association cortex (red). The proximity of colors reflects the similarity of connectivity patterns across cortex. The scale bar reflects z-transformed principal gradient values[41] derived from connectivity matrices using diffusion map embedding. **(B)** The second gradient primarily differentiates the somato/motor and auditory cortex (blue) from the visual system (red). **(C)** The third gradient reflects a network architecture contrasting frontoparietal (red) from default and somato/motor systems (blue). **(D)** Brain organization according to the 7 networks of Yeo et al.[60] overlaid on the AICHA atlas parcels[46].

a bilateral language network organization (μ=9.10^{-3}±0.18), in contrast to strong (μ=1.02±0.13, p<10^{-4}) and mild typical (μ=0.85±0.12, p<10^{-4}) participants. Strong and mild individuals showed no differences (p=0.12). Finally, strength sum and inter-hemispheric connectivity displayed a similar profile across groups, with strong typical ($\mu_{\text{strength sum}}$=12.16±0.39 and μ_r=0.61±0.02) and atypical individuals ($\mu_{\text{strength sum}}$=12.06±0.53 and μ_r=0.61±0.03, all p>0.93) exhibiting a similar profile with significantly larger values than mild individuals ($\mu_{\text{strength sum}}$=9.40±0.35 and μ_r=0.49±0.02, all p<10^{-4}).

Gradients asymmetries and atypical lateralization. We next examined the extent to which the presence of typical and atypical language network lateralization may be evident throughout the functional organization of the cortical sheet. To do so, we took advantage of recent mathematical modeling of the functional topography of the cortex as proposed by Margulies and colleagues[30]. First, functional connectivity matrices (384×384 AICHA parcels[46]) across the full sample were decomposed into components that capture the maximum variance in connectivity. Consistent with prior work[30,47], diffusion map embedding[48] was used to reduce the dimensionality of the connectivity data through the nonlinear projection of the voxels into an embedding space. The resulting functional components or manifolds, here termed gradients, are ordered by the variance they explain in the initial functional connectivity matrix. The present analysis focused on the first three gradients, reflecting divergent spatial patterns of connectivity across the cortex and accounting for 57% of the total variance in cortical connectivity. The first 3 group-level gradients respectively explained 22%, 21%, and 14% of the total variance in the initial matrix of cortical connectivity (Fig. 2).

In line with prior work[30,49–51], one end of the principal gradient of connectivity was anchored in unimodal (somato/motor and visual) regions, while the other end encompassed broad swaths of the asso-

ciation cortex, including aspects of the ventral and dorsal medial prefrontal, posteromedial/retrosplenial, and inferior parietal cortices, representing a functional hierarchy that spans from primary visual and somato/motor areas through the default network[33] (Fig. 2A), which underpins self-referential processing and core aspects of mental simulation[52–54]. Conversely, the second gradient peaked within unimodal networks, revealing a spectrum differentiating the somato/motor and auditory territories from the visual system (Fig. 2B). Lastly, the peak values in the third gradient (Fig. 2C) reflected a distinction between the frontoparietal network, spanning aspects of dorsolateral prefrontal, dorsomedial prefrontal, lateral parietal, and posterior temporal cortices, and the default network[55], placing the brain systems that underpin internally oriented cognition and those that coordinate responses to external task states and support complex cognition[56,57] along distinct ends of this organizational axis.

For each participant, functional network gradient asymmetry values correspond to the difference between the normalized gradient value in the left hemisphere minus the gradient values in the right hemisphere, averaged across all network parcels. Broadly, within the mild and strong typical groups, the first gradient showed a leftward asymmetry for 5 of the 7 networks (average asymmetry values ranging from $\mu_{L\text{-}R(typical)}$=1.11 to $\mu_{L\text{-}R(typical)}$=4.09). The somato/motor network was symmetrical ($\mu_{L\text{-}R(typical)}$=0.01, $CI_{95\%}$=0.24). The control network was strongly right lateralized ($\mu_{L\text{-}R(typical)}$=-6.21, $CI_{95\%}$=0.59) which may align with previous results on attention[58]. Conversely, the second gradient displayed a more heterogeneous pattern. Here, the gradient values within the control network ($\mu_{L\text{-}R(typical)}$=-2.93, $CI_{95\%}$=0.36) were right lateralized, as well with the somato/motor ($\mu_{L\text{-}R(typical)}$=-2.52, $CI_{95\%}$=0.41), limbic ($\mu_{L\text{-}R(typical)}$=-0.63, $CI_{95\%}$=0.48), and default networks ($\mu_{L\text{-}R(typical)}$=-0.54, $CI_{95\%}$=0.26). The visual network was symmetrical ($\mu_{L\text{-}R(typical)}$=-0.24, $CI_{95\%}$=0.29), and the dorsal ($\mu_{L\text{-}R(typical)}$=0.88, $CI_{95\%}$=0.54) and ventral ($\mu_{L\text{-}R(typical)}$=1.26, $CI_{95\%}$=0.45) attentional networks were left lateralized. Finally, the third gradient was primarily right lateralized or symmetrical, with the default ($\mu_{L\text{-}R(typical)}$=-1.20, $CI_{95\%}$=0.73), limbic ($\mu_{L\text{-}R(typical)}$=-2.53, $CI_{95\%}$=0.71) and salience/ventral attention networks ($\mu_{L\text{-}R(typical)}$=-4.26, $CI_{95\%}$=0.63) rightward dominant, and the control ($\mu_{L\text{-}R(typical)}$=-0.77, $CI_{95\%}$=0.90), dorsal attentional ($\mu_{typical}$=-0.61, $CI_{95\%}$=0.67) and somato/motor networks ($\mu_{L\text{-}R(typical)}$=0.34, $CI_{95\%}$=0.34) symmetrical. The visual network was the only leftward lateralized network for the third gradient ($\mu_{L\text{-}R(typical)}$=0.53, $CI_{95\%}$=0.28).

An important unanswered question is whether the broad and dissociable gradient asymmetries observed in individuals with typical and atypical language organization are uniformly distributed across the cortical sheet, or whether they are preferential to specific functional systems. Accordingly, we next tested the extent to which asymmetric profiles of network connectivity are evident within the atypical language participants. Here, mild and strong typical groups were merged into a single typical group[25] and next contrasted with the atypical participants. Broadly, with exception of the limbic network, analyses of covariance revealed a preferential association between language lateralization and the asymmetric organization of association cortex networks, relative to unimodal systems across each of the three gradients (Fig. 3). These data suggest that the lateralization of language functions are carried throughout the '*association centres*' originally hypothesized by Paul Flechsig to underpin higher cortical functions and complex associative processing in humans[59]. See Supplementary Table 7-9 for a full description of all the confound effects on gradient asymmetries, and Supplementary Table 10 alongside Supplementary Figure 1 for a full description of each network gradient asymmetries values for both the typical and atypical groups.

Specifically, in the first gradient, five of the seven networks exhibited a significant main effect of language lateralization (all *ps*<0.002), of which 2 of them exhibited a shift in their lateralization from left to right dominant: the default network ($\mu_{L\text{-}R(atypical)}$=-1.62, $CI_{95\%}$=1.00) and the salience/ventral-attentional network ($\mu_{L\text{-}R(atypical)}$=-1.65, $CI_{95\%}$=1.05). The dorsal-attentional ($\mu_{L\text{-}R(atypical)}$=1.56, $CI_{95\%}$=1.11) and the visual network ($\mu_{L\text{-}R(atypical)}$=0.67, $CI_{95\%}$=0.53) showed a weakened dominance in the left hemisphere. The control network ($\mu_{L\text{-}R(atypical)}$=-9.21, $CI_{95\%}$=1.21) was characterized by an increase in its dominance in favor of the right hemisphere. Those alterations in the hemispheric dominance mainly came from an increase of the gradient value in the right hemisphere for all the networks impacted by the phenotype, except the default network for which the change came from a decrease of the gradient value in the left hemisphere.

Three networks showed a significant impact of language lateralization within the second gradient (all *ps*<0.006), the default ($\mu_{L\text{-}R(atypical)}$=-1.58, $CI_{95\%}$=0.53) and control networks ($\mu_{L\text{-}R(atypical)}$=-4.26, $CI_{95\%}$=0.74) exhibited an increase in their rightward dominance, both coming from a mixed effect of an increase of their gradient values in the right hemisphere and a decrease in the left hemisphere. The salience/ventral-attentional network ($\mu_{L\text{-}R(atypical)}$=-0.17, $CI_{95\%}$=0.92) showed a symmetrical pattern in atypical individuals instead of being leftward dominant, coming from a decrease in its gradient values in the left hemisphere. Of the four remaining networks, two showed rightward lateralization: somato/motor ($\mu_{L\text{-}R(atypical)}$=-1.28, $CI_{95\%}$=1.28), and limbic ($\mu_{L\text{-}R(atypical)}$=-1.77, $CI_{95\%}$=0.99), and the two last

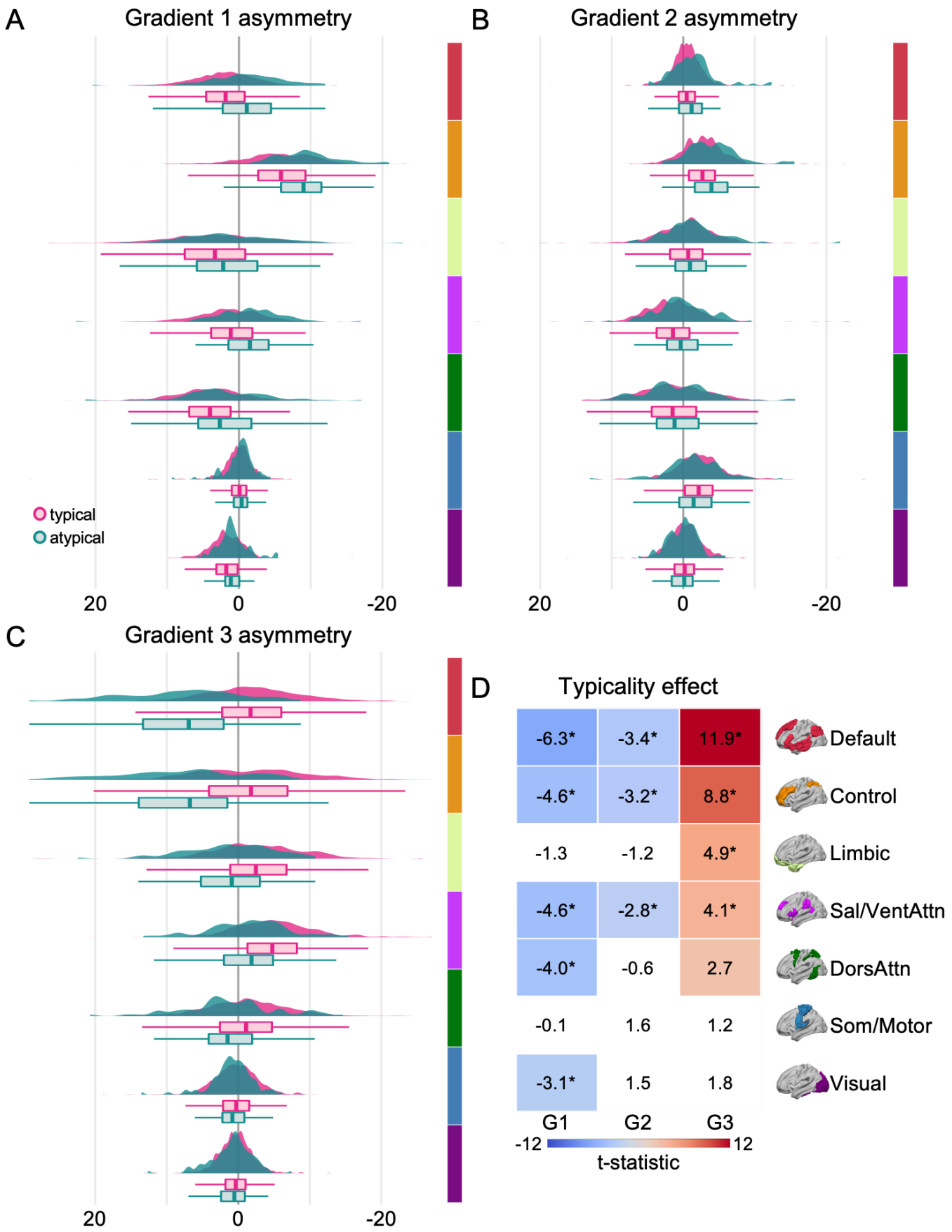

Fig. 3 | Language lateralization is evident throughout the macroscale organization of the cortex. (A-C) Network-level asymmetry (left *minus* right hemisphere) of the first three gradients for each language lateralization group. Colors reflect brain organization according to the 7 networks[60] averaged across corresponding AICHA atlas parcels[46]. Graphs display the density and boxplot (lower and upper hinges correspond to the 1st and 3rd quartiles, the middle line the median) of individual gradient asymmetry values for the typical (magenta) and atypical (teal) groups. **(D)** The 2D grid displays the extent of language lateralization for each gradient and functional network. Values reflect the post-hoc t-statistic of the typicality main effect from ANCOVA. Colored cells display significant uncorrected effects ($p \leq 0.05$). Cells with a star are significant after Bonferroni correction for network number ($p \leq 0.007$). In these analyses, each individual gradient has been scaled between 0 and 100.

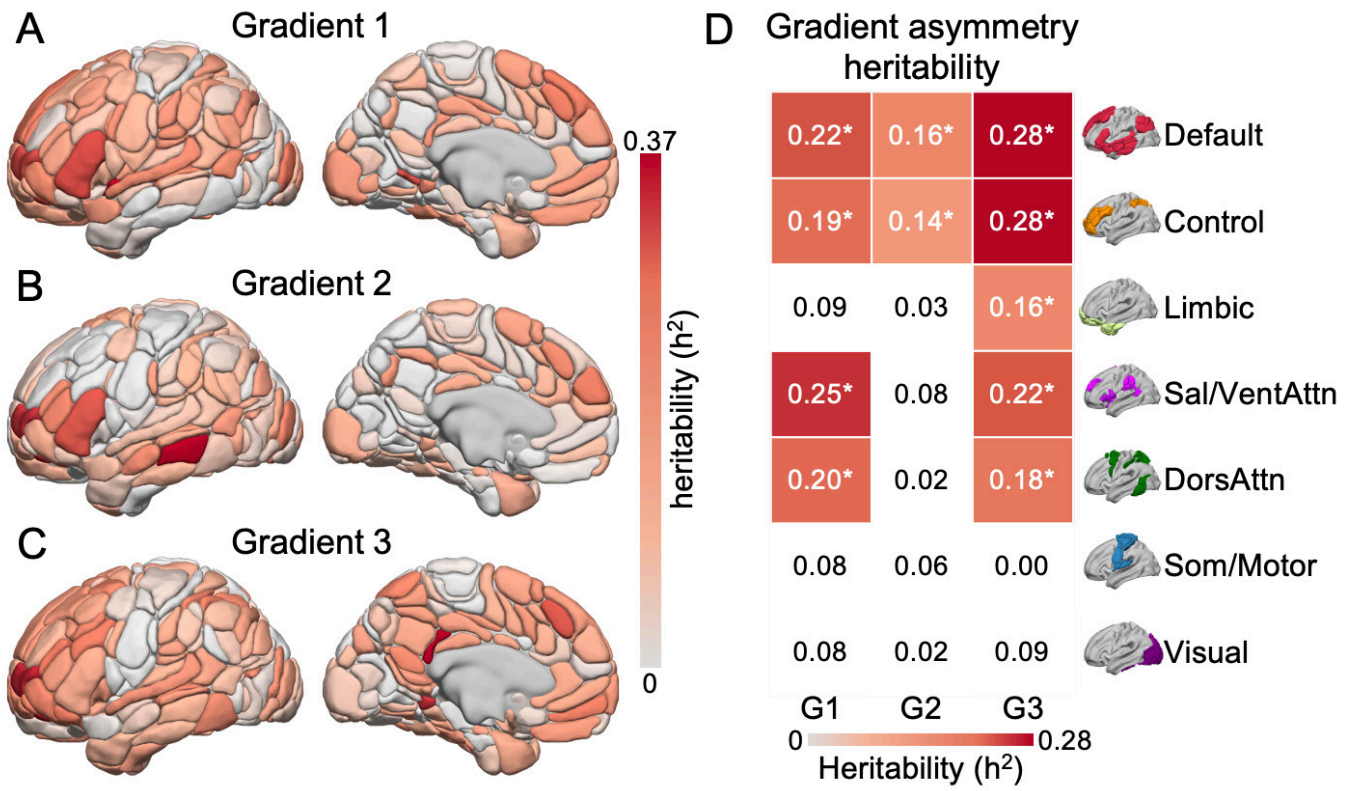

Fig. 4 | The heritability of gradient asymmetry is evident in the macroscopic organization of the cortex. (A-C) Regional-level heritability of the asymmetry (left minus right hemisphere) of the first three gradients. Warmer colors (solid red) indicate higher heritability of gradient asymmetry, for instance reflecting greater similarity among twins and siblings than unrelated individuals. **(D)** The 2D grid displays the extent of heritability of gradient asymmetry for each gradient and functional network. Values reflect the heritability of gradient asymmetry. Heritability of network asymmetry was estimated across 7 canonical functional networks using SOLAR[67]. Colored cells reflect networks with significant heritability of gradient laterality ($p \leq 0.05$ uncorrected). Cells with a star are those remaining significant after Bonferroni correction ($p \leq 0.007$).

Heritability of language lateralization and gradient asymmetry. Population-based neuroimaging studies have revealed the influence of genetic factors on the connectivity strength[61], size, and spatial organization[62] of large-scale cortical networks. However, although prior work has begun to catalog the evolution[63], development[47,64], and organization[65,66] of the brain's functional architecture, the role of genetics in sculpting the lateralization of cognitive functions and associated asymmetries in the macroscale organization of cortex has yet to be quantified. Here, to advance our understanding of the biological bases of hemispheric specialization, we worked to determine heritable sources of variation that may govern the lateralization of both localized language functions and functional gradient asymmetries across the cortical sheet.

Leveraging a nonlinear multidimensional estimation of heritability[62], our analyses suggest that both the lateralization of the language network, as assessed through the hierarchical classification approach (h^2=11.2%, SE=6%, p=0.038), and the hemispheric asymmetries in gradient organization, reflecting the difference in gradient values between the left and right hemisphere (Supplementary Table 11, G1: 14.4%, SE=6%, p=0.007; G2: 2.0%, SE=5%, p=0.36; G3: 24.0%, SE=6%, $p<1.10^{-4}$), are under genetic control. Heritability of gradient asymmetry values for each network was estimated using sequential oligogenic linkage analysis routines (SOLAR[67]) and covaried for age, sex, age^2, age × sex, age^2 × sex, handedness, and FreeSurfer-derived intracranial volume. Prior work examining connectivity strengths and the network topographies indicates reduced heritability in the size[62] and connectivity strength[61] of heteromodal association networks, relative to unimodal sensory/motor cortex. In contrast, with the exception of the limbic network, the present analyses revealed the influence of genetic factors on the gradient asymmetries across each association cortex network. Notably, genetic factors did not significantly account for the lateralization of gradient values within somato/motor and visual territories and heritability was significantly greater (Fig. 4; p<0.001) within heteromodal (h^2: μ=18.5%, SD=7.7%) association cortices than within unimodal networks (h^2: μ=5.5%, SD=3.8%). Overall, these data reveal the substantial influence of genetic factors on the lateralization of both specific cognitive functions and the broad functional organization of the cortex. These results are consistent with the hypothesis that neuronal asymmetries likely devel-

oped under phylogenetic pressure, and therefore possess a genetic basis[68].

Discussion

Our present study reveals that asymmetrical language network organization is broadly reflected throughout the global connectivity structure of the cerebral cortex. Using task-evoked and resting-state data, we identify a pattern of atypical language network lateralization and corresponding alterations in functional coupling across the cortical sheet in ~8 percent of individuals. These group-level changes in connectivity are preferential to transmodal association cortex and heritable, providing evidence that both the lateralization of the cortical territories supporting language and the associated functional processing streams they are embedded within are under genetic control. Together, this work advances our understanding of the relationship between the localized hemispheric specialization of specific behaviors and the hierarchical functional axes that capture the topographic organization of large-scale cortical networks.

Hemispheric specialization reflects a core property of human cognition and a marker of successful development. In most individuals, the left hemisphere is specialized for language and motor control of their dominant hand, whereas the right hemisphere plays a preferential role in visuospatial processing[69,70]. Across development, the maturation of lateralized functions is associated with improved visuospatial and language abilities and enhanced cognitive efficiency[71,72]. Although the precise timing of these developmental cascades remains largely unknown[14,15], some markers of lateralization are already apparent during gestation, for instance the leftward asymmetrical folding of the Sylvian fissure[73]. At birth, intra-hemispheric white matter connectivity across the language network is reduced in favor of strong inter-hemispheric coordination[74], an organizational property that is consistent with the presence of prominent homotopic intrinsic connectivity from 3 to 6 months of life[75]. Suggesting a complex developmental picture that is sensitive to task state, when newborns are presented with spoken words they exhibit a left-lateralized asymmetric response, whereas brain connectivity at rest remains evenly distributed across hemispheres[76]. Although multiple factors appear to contribute to the emergence of lateralized functions[77], atypical language organization and more globally atypical functional lateralization are preferentially evident in individuals with neurodevelopmental, psychiatric, and/or neurological disorders[11,21,78], such as autism[79–82] and schizophrenia[83,84]. Here, in a population of healthy young adults, we observed atypical lateralization in a sizable minority of the study sample. Critically, although individuals with language and/or cognitive impairments often present with altered cerebral lateralization, the vast majority of people with atypical language lateralization have no corresponding cognitive deficits[85,86], or exhibit slightly lower visuospatial and verbal memory performance compared to strong leftward lateralized individuals[25]. As such, understanding the interactions linking the biological underpinnings of language lateralization, cognition, and illness risk would have significant implications for both developmental biology and cognitive neuroscience[21].

The cerebral cortex is composed of areal parcels, embedded within a set of distributed large-scale networks, and positioned within corresponding processing streams[1,32,33,87]. The parallel and interdigitated organization of cortical networks suggests that the language system may impinge upon, and be influenced by, putatively distinct yet spatially adjacent networks[88]. Extending upon recent evidence indicating that asymmetries in regional brain anatomy are reflected throughout the entire brain[89,90], our analyses revealed a relationship between the lateralizations of language functions and the sweeping functional gradients that capture the topography of large-scale networks across cortex. Of note, across all three gradients the observed differences between the typical and atypical groups were preferential to association networks. Over the course of vertebrate evolution, the evolutionary enlargement of the cortical mantle in primates has been preferentially localized within spatially distributed aspects of association cortex, relative to the primary and secondary sensory systems, perhaps allowing for the development of novel capabilities independent from the primary senses[63,91]. The present profile of results is consistent with literature indicating hemispheric asymmetries for both language and attentional allocation as well as theories suggesting that phylogenetically expanded aspects of cortex, for example inferior parietal lobule, reflect the cortical territories with the most prominent structural and functional asymmetries in humans[92]. Critically, our analyses cannot establish the specific biological cascades that influence the emergence of atypical language laterality or corresponding shifts in the broad functional architecture of cortex. Rather, these data highlight the importance of future work to identify underlying processes that contribute to the development of functional asymmetries across the cortical sheet and associated hemispheric differences in information processing. Across each of the three main gradients, the lateralization of language appeared to preferentially reverberate throughout the functional architecture of association cortex. Although speculative, the present analyses suggest that the lateralization of isolated functions, such as language, may be tightly tied to the lateralization of

a host of other seemingly independent processes.

The genetic origin of language capacities[93] and other properties of hemispheric specialization reflect a fundamental question in cognitive neuroscience with clear relevance for the study of both health and disease[12]. Prior work indicates that intrinsic connectivity between language related regions[94], as well as evoked brain activations during language tasks[95], are heritable. Our present analyses indicate a clear genetic basis for population-level patterns of language lateralization and corresponding features of cortical organization. Here, the heritability of gradient asymmetries were evident across the cortical sheet, preferential to functional networks within association territories. Prior work has revealed core principles that govern the evolution, development, and organization of large-scale brain networks. Broadly, in contrast to our present work, these data have suggested relaxed genetic control of association cortices relative to primary sensory/motor regions[62]. A profile of heritability that is consistent with the presence of increased population-level variability in functional connectivity[96], relative network sizes, and topographic network similarity in association relative to unimodal cortex[62,97–99]. The discovery of the increased influence of genetic factors on the gradient asymmetries across each association cortex network raises the possibility that, despite the broadly reduced heritability of association cortex functions, features of brain lateralization remain preferentially influenced by genetics. One speculation is that our present results reflect two partially distinct developmental paths, first an initial genetically mediated developmental cascade biasing fundamental aspects of brain lateralization. Second, once the genetically mediated plan is laid out, the subsequent protracted development of association cortex functions provides for a period of prolonged plasticity and increased sensitivity to environmental inputs[100,101].

Although the present results provide evidence that atypical language network organization is linked to widespread properties of cortical organization, there are several limitations with the present approach. First, the causal pathways linking the lateralization of the putatively distinct cognitive processes with broad features of brain functioning remain to be established. In the present data we are unable, for instance, to examine atypicalities in the lateralization of attentional processes. Additionally, given the cross sectional nature of the present data, we are not able to establish the developmental course linking atypicality in language lateralization with the development of global brain architecture. As such, the manner through which lateralized functions impinge upon, and are in turn influenced by, other properties of brain organization across development remains an open question. Finally, from a clinical perspective, the presence of aphasias and corresponding shifts in the global functional architecture of cortex have yet to be established[102,103].

The extent to which the lateralization of specific cognitive functions may be evident across the macroscale organizational properties of the cortical sheet is a central question across the brain sciences. The present results demonstrate that asymmetric language network organization is carried throughout association cortex. While the exact determinants of lateralization mechanisms are still unknown, both the hemispheric specialization of language and corresponding asymmetries across the sweeping functional gradients that span cerebral cortex were found to be heritable. Here, the lateralization of heteromodal association cortex networks under increased genetic control, relative unimodal networks. The further study of this entangled relationship between language lateralization and broader properties of functional network organization has the potential to shed light on the phenomenon of cerebral dominance thought to underpin sophisticated cognition in humans[104] as well as neuropsychiatric and neurological disorders with known alterations in brain laterality[105,106].

References

1. Mesulam, M. M. Large-scale neurocognitive networks and distributed processing for attention, language, and memory. Ann. Neurol. 28, 597–613 (1990).
2. Fuster, J. M. Linkage at the top. Neuron 21, 1223–1224 (1998).
3. Stark, D. E. et al. Regional variation in interhemispheric coordination of intrinsic hemodynamic fluctuations. J. Neurosci. 28, 13754–13764 (2008).
4. Mancuso, L. et al. The homotopic connectivity of the functional brain: a meta-analytic approach. Sci. Rep. 9, 3346 (2019).
5. Menon, V. Large-scale functional brain organization. in Brain Mapping 449–459 (Elsevier, 2015).
6. Heger, P., Zheng, W., Rottmann, A., Panfilio, K. A. & Wiehe, T. The genetic factors of bilaterian evolution. (2020) doi:10.7554/eLife.45530.
7. Güntürkün, O. & Ocklenburg, S. Ontogenesis of Lateralization. Neuron 94, 249–263 (2017).
8. Labache, L. et al. A SENtence Supramodal Areas AtlaS (SENSAAS) based on multiple task-induced activation mapping and graph analysis of intrinsic connectivity in 144 healthy right-handers. Brain Struct. Funct. 224, 859–882 (2019).
9. Oppenheimer, J. M. Studies of brain asymmetry: historical perspective. Ann. N. Y. Acad. Sci. 299, 4–17 (1977).
10. Finger, S. & Roe, D. Gustave Dax and the early history of cerebral dominance. Arch. Neurol. 53, 806–813 (1996).
11. Vingerhoets, G. Phenotypes in hemispheric

functional segregation? Perspectives and challenges. Phys. Life Rev. 30, 1–18 (2019).
12. Francks, C. In search of the biological roots of typical and atypical human brain asymmetry: Comment on 'Phenotypes in hemispheric functional segregation? Perspectives and challenges' by Guy Vingerhoets. Physics of life reviews vol. 30 22–24 (2019).
13. Thiebaut de Schotten, M., Friedrich, P. & Forkel, S. J. One size fits all does not apply to brain lateralisation: Comment on 'Phenotypes in hemispheric functional segregation? Perspectives and challenges' by Guy Vingerhoets. Physics of life reviews vol. 30 30–33 (2019).
14. Tzourio-Mazoyer, N., Zago, L., Cochet, H. & Crivello, F. Development of handedness, anatomical and functional brain lateralization. Handb. Clin. Neurol. 173, 99–105 (2020).
15. McManus, C. Cerebral Polymorphisms for Lateralisation: Modelling the Genetic and Phenotypic Architectures of Multiple Functional Modules. Symmetry 14, 814 (2022).
16. Geschwind, N. The organization of language and the brain. Science 170, 940–944 (1970).
17. Price, C. J. A review and synthesis of the first 20 years of PET and fMRI studies of heard speech, spoken language and reading. Neuroimage 62, 816–847 (2012).
18. Roger, E. et al. Unraveling the functional attributes of the language connectome: crucial subnetworks, flexibility and variability. Neuroimage 119672 (2022).
19. Hécaen, H. & Sauguet, J. Cerebral Dominance in Left-Handed Subjects. Cortex vol. 7 19–48 Preprint at https://doi.org/10.1016/s0010-9452(71)80020-5 (1971).
20. Isaacs, K. L., Barr, W. B., Nelson, P. K. & Devinsky, O. Degree of handedness and cerebral dominance. Neurology 66, 1855–1858 (2006).
21. Bishop, D. V. M. Cerebral asymmetry and language development: cause, correlate, or consequence? Science 340, 1230531 (2013).
22. Ocklenburg, S., Beste, C., Arning, L., Peterburs, J. & Güntürkün, O. The ontogenesis of language lateralization and its relation to handedness. Neurosci. Biobehav. Rev. 43, 191–198 (2014).
23. Olulade, O. A. et al. The neural basis of language development: Changes in lateralization over age. Proc. Natl. Acad. Sci. U. S. A. 117, 23477–23483 (2020).
24. Carey, D. P. & Johnstone, L. T. Quantifying cerebral asymmetries for language in dextrals and adextrals with random-effects meta analysis. Front. Psychol. 5, 1128 (2014).
25. Labache, L. et al. Typical and atypical language brain organization based on intrinsic connectivity and multitask functional asymmetries. Elife 9, (2020).
26. Mazoyer, B. et al. Gaussian Mixture Modeling of Hemispheric Lateralization for Language in a Large Sample of Healthy Individuals Balanced for Handedness. PLoS ONE vol. 9 e101165 (2014).
27. Knecht, S. et al. Language lateralization in healthy right-handers. Brain 123 (Pt 1), 74–81 (2000).
28. Doucet, G. E., Lee, W. H. & Frangou, S. Evaluation of the spatial variability in the major resting-state networks across human brain functional atlases. Hum. Brain Mapp. 40, 4577–4587 (2019).
29. Gordon, E. M. et al. Generation and Evaluation of a Cortical Area Parcellation from Resting-State Correlations. Cereb. Cortex 26, 288–303 (2016).
30. Margulies, D. S. et al. Situating the default-mode network along a principal gradient of macroscale cortical organization. Proc. Natl. Acad. Sci. U. S. A. 113, 12574–12579 (2016).
31. Mesulam, M.-M. Principles of Behavioral and Cognitive Neurology. (Oxford University Press, 2000).
32. Sydnor, V. J. et al. Neurodevelopment of the association cortices: Patterns, mechanisms, and implications for psychopathology. Neuron 109, 2820–2846 (2021).
33. Huntenburg, J. M., Bazin, P.-L. & Margulies, D. S. Large-Scale Gradients in Human Cortical Organization. Trends Cogn. Sci. 22, 21–31 (2018).
34. Sepulcre, J. et al. The organization of local and distant functional connectivity in the human brain. PLoS Comput. Biol. 6, e1000808 (2010).
35. Reardon, P. K. et al. Normative brain size variation and brain shape diversity in humans. Science 360, 1222–1227 (2018).
36. Paquola, C. et al. A multi-scale cortical wiring space links cellular architecture and functional dynamics in the human brain. PLoS Biol. 18, e3000979 (2020).
37. Goulas, A., Zilles, K. & Hilgetag, C. C. Cortical Gradients and Laminar Projections in Mammals. Trends Neurosci. 41, 775–788 (2018).
38. Richiardi, J. et al. BRAIN NETWORKS. Correlated gene expression supports synchronous activity in brain networks. Science 348, 1241–1244 (2015).
39. Burt, J. B. et al. Hierarchy of transcriptomic specialization across human cortex captured by structural neuroimaging topography. Nat. Neurosci. 21, 1251–1259 (2018).
40. Anderson, K. M. et al. Transcriptional and imaging-genetic association of cortical interneurons, brain function, and schizophrenia risk. Nat. Commun. 11, 2889 (2020).
41. Gonzalez Alam, T. R. D. J. et al. A tale of two gradients: differences between the left and right hemispheres predict semantic cognition. Brain Struct. Funct. 227, 631–654 (2022).
42. Liang, X. et al. Sex-related human brain asymmetry in hemispheric functional gradients. Neuroimage 229, 117761 (2021).
43. Van Essen, D. C. et al. The WU-Minn Human Connectome Project: an overview. Neuroimage 80, 62–79 (2013).
44. Barch, D. M. et al. Function in the human connectome: task-fMRI and individual differences in behavior. Neuroimage 80, 169–189 (2013).
45. Mazoyer, B. et al. BIL&GIN: A neuroimaging, cognitive, behavioral, and genetic database for the study of human brain lateralization. Neuroimage 124, 1225–1231 (2016).
46. Joliot, M. et al. AICHA: An atlas of intrinsic connectivity of homotopic areas. J. Neurosci. Methods 254, 46–59 (2015).
47. Dong, H.-M., Margulies, D. S., Zuo, X.-N. &

Holmes, A. J. Shifting gradients of macroscale cortical organization mark the transition from childhood to adolescence. Proc. Natl. Acad. Sci. U. S. A. 118, (2021).
48. Coifman, R. R. & Lafon, S. Diffusion maps. Appl. Comput. Harmon. Anal. 21, 5–30 (2006).
49. Bernhardt, B. C., Smallwood, J., Keilholz, S. & Margulies, D. S. Gradients in brain organization. Neuroimage 251, 118987 (2022).
50. Hong, S.-J. et al. Toward a connectivity gradient-based framework for reproducible biomarker discovery. Neuroimage 223, 117322 (2020).
51. Mckeown, B. et al. The relationship between individual variation in macroscale functional gradients and distinct aspects of ongoing thought. Neuroimage 220, 117072 (2020).
52. Buckner, R. L., Andrews-Hanna, J. R. & Schacter, D. L. The brain's default network: anatomy, function, and relevance to disease. Ann. N. Y. Acad. Sci. 1124, 1–38 (2008).
53. Buckner, R. L. & DiNicola, L. M. The brain's default network: updated anatomy, physiology and evolving insights. Nat. Rev. Neurosci. 20, 593–608 (2019).
54. Mazoyer, B. et al. Cortical networks for working memory and executive functions sustain the conscious resting state in man. Brain Res. Bull. 54, 287–298 (2001).
55. Smallwood, J. et al. The default mode network in cognition: a topographical perspective. Nat. Rev. Neurosci. 22, 503–513 (2021).
56. Cole, M. W. et al. Multi-task connectivity reveals flexible hubs for adaptive task control. Nat. Neurosci. 16, 1348–1355 (2013).
57. Samara, A., Eilbott, J., Margulies, D. S., Xu, T. & Vanderwal, T. Cortical gradients during naturalistic processing are hierarchical and modality-specific. bioRxiv (2022) doi:10.1101/2022.10.15.512379.
58. Karolis, V. R., Corbetta, M. & Thiebaut de Schotten, M. The architecture of functional lateralisation and its relationship to callosal connectivity in the human brain. Nat. Commun. 10, 1417 (2019).
59. Flechsig, P. Die Localisation der geistigen Vorgänge insbesondere der Sinnesempfindungen des Menschen: Vortrag, gehalten auf der 68. Versammlung Deutscher Naturforscher und Ärzte zu Frankfurt. (de Gruyter, 2021). doi:10.1515/9783112366400.
60. Yeo, B. T. T. et al. The organization of the human cerebral cortex estimated by intrinsic functional connectivity. J. Neurophysiol. 106, 1125–1165 (2011).
61. Ge, T., Holmes, A. J., Buckner, R. L., Smoller, J. W. & Sabuncu, M. R. Heritability analysis with repeat measurements and its application to resting-state functional connectivity. Proc. Natl. Acad. Sci. U. S. A. 114, 5521–5526 (2017).
62. Anderson, K. M. et al. Heritability of individualized cortical network topography. Proc. Natl. Acad. Sci. U. S. A. 118, (2021).
63. Chin, R., Chang, S. W. C. & Holmes, A. J. Beyond cortex: The evolution of the human brain. Psychol. Rev. (2022) doi:10.1037/rev0000361.
64. Fair, D. A. et al. Development of distinct control networks through segregation and integration. Proc. Natl. Acad. Sci. U. S. A. 104, 13507–13512 (2007).
65. Schaefer, A. et al. Local-Global Parcellation of the Human Cerebral Cortex from Intrinsic Functional Connectivity MRI. Cereb. Cortex 28, 3095–3114 (2018).
66. Glasser, M. F. et al. A multi-modal parcellation of human cerebral cortex. Nature 536, 171–178 (2016).
67. Almasy, L. & Blangero, J. Multipoint quantitative-trait linkage analysis in general pedigrees. Am. J. Hum. Genet. 62, 1198–1211 (1998).
68. Manns, M. It is not just in the genes. Symmetry 13, 1815 (2021).
69. Hervé, P.-Y., Zago, L., Petit, L., Mazoyer, B. & Tzourio-Mazoyer, N. Revisiting human hemispheric specialization with neuroimaging. Trends Cogn. Sci. 17, 69–80 (2013).
70. Thiebaut de Schotten, M. et al. A lateralized brain network for visuospatial attention. Nat. Neurosci. 14, 1245–1246 (2011).
71. Everts, R. et al. Strengthening of laterality of verbal and visuospatial functions during childhood and adolescence. Hum. Brain Mapp. 30, 473–483 (2009).
72. Gotts, S. J. et al. Two distinct forms of functional lateralization in the human brain. Proc. Natl. Acad. Sci. U. S. A. 110, E3435–44 (2013).
73. Hill, J. et al. A surface-based analysis of hemispheric asymmetries and folding of cerebral cortex in term-born human infants. J. Neurosci. 30, 2268–2276 (2010).
74. Perani, D. et al. Neural language networks at birth. Proc. Natl. Acad. Sci. U. S. A. 108, 16056–16061 (2011).
75. Homae, F. et al. Development of global cortical networks in early infancy. J. Neurosci. 30, 4877–4882 (2010).
76. Xiao, Y. et al. Development of the Intrinsic Language Network in Preschool Children from Ages 3 to 5 Years. PLoS One 11, e0165802 (2016).
77. Liu, H., Stufflebeam, S. M., Sepulcre, J., Hedden, T. & Buckner, R. L. Evidence from intrinsic activity that asymmetry of the human brain is controlled by multiple factors. Proc. Natl. Acad. Sci. U. S. A. 106, 20499–20503 (2009).
78. Mundorf, A. & Ocklenburg, S. The Clinical Neuroscience of Lateralization. Preprint at https://doi.org/10.4324/9781003082507 (2021).
79. Knaus, T. A. et al. Language laterality in autism spectrum disorder and typical controls: a functional, volumetric, and diffusion tensor MRI study. Brain Lang. 112, 113–120 (2010).
80. Whitehouse, A. J. O. & Bishop, D. V. M. Cerebral dominance for language function in adults with specific language impairment or autism. Brain 131, 3193–3200 (2008).
81. Floris, D. L. et al. Atypical Brain Asymmetry in Autism-A Candidate for Clinically Meaningful Stratification. Biol Psychiatry Cogn Neurosci Neuroimaging 6, 802–812 (2021).
82. Jouravlev, O. et al. Reduced Language Lateralization in Autism and the Broader Autism Phenotype as Assessed with Robust Individual-Subjects Analyses. Autism Res. 13, 1746–1761

(2020).
83. Zeev-Wolf, M., Goldstein, A., Levkovitz, Y. & Faust, M. Fine-coarse semantic processing in schizophrenia: a reversed pattern of hemispheric dominance. Neuropsychologia 56, 119–128 (2014).
84. Dollfus, S. et al. Atypical hemispheric specialization for language in right-handed schizophrenia patients. Biol. Psychiatry 57, 1020–1028 (2005).
85. Knecht, S. et al. Behavioural relevance of atypical language lateralization in healthy subjects. Brain 124, 1657–1665 (2001).
86. Cai, Q., Van der Haegen, L. & Brysbaert, M. Complementary hemispheric specialization for language production and visuospatial attention. Proc. Natl. Acad. Sci. U. S. A. 110, E322–30 (2013).
87. Goldman-Rakic, P. S. Topography of cognition: parallel distributed networks in primate association cortex. Annu. Rev. Neurosci. 11, 137–156 (1988).
88. Braga, R. M., DiNicola, L. M., Becker, H. C. & Buckner, R. L. Situating the left-lateralized language network in the broader organization of multiple specialized large-scale distributed networks. J. Neurophysiol. 124, 1415–1448 (2020).
89. Saltoun, K. et al. Dissociable brain structural asymmetry patterns reveal unique phenome-wide profiles. Nat Hum Behav (2022) doi:10.1038/s41562-022-01461-0.
90. Chen, Y.-C. et al. The individuality of shape asymmetries of the human cerebral cortex. Elife 11, (2022).
91. DiNicola, L. M. & Buckner, R. L. Precision Estimates of Parallel Distributed Association Networks: Evidence for Domain Specialization and Implications for Evolution and Development. Curr Opin Behav Sci 40, 120–129 (2021).
92. Hartwigsen, G., Bengio, Y. & Bzdok, D. How does hemispheric specialization contribute to human-defining cognition? Neuron 109, 2075–2090 (2021).
93. Fisher, S. E. & Vernes, S. C. Genetics and the language sciences. Annu. Rev. Linguist. 1, 289–310 (2015).
94. Mekki, Y. et al. The genetic architecture of language functional connectivity. Neuroimage 249, 118795 (2022).
95. Le Guen, Y., Amalric, M., Pinel, P., Pallier, C. & Frouin, V. Shared genetic aetiology between cognitive performance and brain activations in language and math tasks. Sci. Rep. 8, 17624 (2018).
96. Mueller, S. et al. Individual variability in functional connectivity architecture of the human brain. Neuron 77, 586–595 (2013).
97. Gu, Z., Jamison, K. W., Sabuncu, M. R. & Kuceyeski, A. Heritability and interindividual variability of regional structure-function coupling. Nat. Commun. 12, 4894 (2021).
98. Arnatkeviciute, A. et al. Genetic influences on hub connectivity of the human connectome. Nat. Commun. 12, 4237 (2021).
99. Valk, S. L. et al. Genetic and phylogenetic uncoupling of structure and function in human transmodal cortex. Nat. Commun. 13, 2341 (2022).
100. Morillon, B. et al. Neurophysiological origin of human brain asymmetry for speech and language. Proc. Natl. Acad. Sci. U. S. A. 107, 18688–18693 (2010).
101. Skeide, M. A. & Friederici, A. D. The ontogeny of the cortical language network. Nat. Rev. Neurosci. 17, 323–332 (2016).
102. Matchin, W. et al. The Wernicke conundrum revisited: evidence from connectome-based lesion-symptom mapping. Brain 145, 3916–3930 (2022).
103. Mesulam, M.-M. et al. Modularity and granularity across the language network-A primary progressive aphasia perspective. Cortex 141, 482–496 (2021).
104. McManus, I. C. Handedness, cerebral lateralization, and the evolution of language. in (Oxford University Press, 2000).
105. Schijven, D. et al. Large-scale analysis of structural brain asymmetries in schizophrenia via the ENIGMA consortium. bioRxiv (2022) doi:10.1101/2022.03.01.22271652.
106. Sun, T. & Walsh, C. A. Molecular approaches to brain asymmetry and handedness. Nat. Rev. Neurosci. 7, 655–662 (2006).

Methods

HCP participants. The study sample was part of the S1200 Release (updated April 2018) of the WU-Minn Human Connectome Project (HCP) database that has been fully described elsewhere[43]. From 1206 healthy participants, participants with fully completed 3T language and 3T resting-state fMRI protocols were selected, resulting in a total of 995 participants (477 women). The mean educational level of participants was 14.97 years (SD=1.77 years). The sample mean age was 28.70 years (SD=3.71 years). Participants' handedness was defined based on the manual preference strength assessed with the Edinburgh inventory[107]: participants with a score below 30 were considered left-handers[108,109], right-handers otherwise. The sample contained 110 left-handed participants (50 women), leading to a sample broadly representative of the general population[109,110]. Data collection was approved by a consortium of institutions institutional review boards (IRBs) in the United States and Europe, led by Washington University (St Louis) and the University of Minnesota (WU-Minn HCP Consortium). The current study was approved by the Yale University IRB.

MRI Data Preprocessing. HCP datasets used include two main imaging sessions. Data were acquired using multiband echo-planar imaging (EPI) on a customized Siemens 3T MRI scanner (Skyra system). Structural data consisted of one 0.7mm isotropic scan. (1) Two sessions (REST1 and REST2) of resting-state fMRI (rs-fMRI), where each session comprised two runs (left-to-right, and right-to-left, phase encoding) of 14min and 33s each (repetition time (TR)=720ms, echo time (TE)=33.1ms, voxel dimension: 2mm isotropic). Details on rs-fMRI can be

found elsewhere[111]. (2) Task fMRI (t-fMRI) data were acquired using the identical multiband EPI sequence as the rs-fMRI session. Among the 7 contrasts, only the Story *minus* Math contrast was used. Details on the protocol are available elsewhere[44]. The language-related protocol was developed by Binder and colleagues[112]. Briefly, the contrast consisted of comparing comprehension of brief narratives (Story task) with a semantically shallow control task involving serial arithmetic (Math task). Two runs were performed each consisting of 4 blocks of a Story interleaved with 4 blocks of a Math task. Each run was 3.8min long.

Minimally preprocessed volumetric rs- and t-fMRI data were sourced from the online HCP repository through Amazon Web Services (AWS). Details of the minimal preprocessing pipeline can be found elsewhere[113]. The R library *neurohcp*[114] was used to interface AWS S3 bucket (R package version: 0.9.0). The R library *RNifti*[115] was used to read and handle the fMRI data (R package version: 1.3.1).

The 995 individuals have been coregistered using MSM-All pipeline. t-fMRI data are represented in the HCP 32k_LR MNI surface space[116], since volume-smoothed level 2 t-fMRI analysis results are no longer being distributed. rs-fMRI data are represented in the MNI volumetric space.

Language Atlas Statistics. Preprocessed data were analyzed to compute 5 functional features characterizing the high-order language network. These 5 features have been previously shown to accurately determine the language network typicality[25].

The high-order language atlas has been fully described elsewhere[8]. Briefly, 18 regions of interest corresponding to the core language network have been selected from the language atlas. The core language network corresponded to a set of heteromodal brain regions significantly involved, leftward asymmetrical across 3 language contrasts (listening to, reading, and producing sentences), and intrinsically connected. It should be noted that the language atlas was based on the AICHA atlas, a functional brain atlas optimized for the study of functional brain asymmetries[46].

First, two of the 5 features were computed from the t-fMRI data. For each individual, the native volumetric language atlas has been mapped to the closest mid-thickness surface vertex using tools from the HCP workbench[117]. The surface language atlas was then used as a binary mask to estimate the average BOLD signal variation of language networks in both hemispheres for the Story *minus* Math contrast. The average asymmetry of activations was then measured by computing the difference between the left and right hemispheres (left-right). The same process has been repeated to estimate the average asymmetry at the hub level. A description of language hubs can be found in Labache and colleagues[8]. Briefly, the language network hubs corresponded to the inferior frontal gyrus (Broca's area) and to the posterior aspect of the superior temporal sulcus (corresponding to Wernicke's area).

Second, the 3 other features were computed from the rs-fMRI data. For each of 4 rs-fMRI scans, each individual and each of 18 language regions, an individual BOLD rs-fMRI time series was computed by averaging the BOLD fMRI time series of all voxels located within the region's volume. An intrinsic connectivity matrix was then calculated for each of 995 individuals and scans. The intrinsic connectivity matrix off-diagonal elements were the Pearson correlation coefficients between the rs-fMRI time series of region pairs. For each individual, the 4 connectivity matrices were *z*-transformed prior to being averaged and *r*-transformed with a hyperbolic tangent function. The 4 scans were averaged to increase the signal-to-noise ratio and reliability for generating individual functional connectivity matrices[118]. For each individual and each region, the strength, or centrality degree, was computed in each hemisphere. The strength was calculated as the sum of the positive correlations existing between one region and all the 18 others. Strength values were then averaged across the 18 regions of the same hemisphere and the resulting left and right averaged strength values were summed. The left minus right differences were also computed. Finally, the inter-hemispheric connectivity strength was estimated in each individual by averaging across the 18 region pairs of the *z*-transformed intrinsic correlation coefficient between homotopic regions. The strength sum, the strength asymmetry, and the inter-hemispheric connectivity strength from the last set of 3 variables.

Connectivity Embedding. For each participant, values were obtained for the first 3 functional gradients. The gradients reflect participant connectivity matrices, reduced in their dimensionality through the approach of Margulies and colleagues[30]. Functional gradients reflect the topographical organization of cortex in terms of sensory integration flow as described by Mesulam[119]. Gradients were computed using Python[120] (Python version: 3.8.10) and the *BrainSpace* library[121] (Python library version: 0.1.3). Gradients computed at both the regional and vertex level showed similar performance[121].

Average region-level functional connectivity matrices of the 4 scans were generated for each individual across the entire cortex (*i.e.* 384 AICHA brain regions, same process as for the language connectivity matrices). Consistent with prior work, the top 10% connections of each region were retained, and other elements in the matrix were set to 0 to en-

force sparsity[30,47]. The normalized angle distance between any two rows of a matrix was calculated to obtain a symmetrical similarity matrix. Diffusion map embedding[48,122,123] was implemented on the similarity matrix to derive the first 3 gradients. Note that the individual-level gradients were aligned using Procrustes rotation ($N_{iterations}$=10) to the corresponding group-level gradient. This alignment procedure was used to improve the similarity of the individual-level gradients to those from the prior literature. Min-max normalization (0-100) was performed at the individual level for the whole brain[41].

To keep the subsequent analysis circumscribed to large-scale network brain organization, gradients values have been averaged, for each participant, according to each of the 7 networks described by Yeo and colleagues[60]. Prior to the averaging step, each AICHA region has been assigned to one of the 7 networks based on its spatial overlap with a given network. Gradient asymmetry was then computed for each participant and region. For a given network, gradient asymmetry corresponded to the difference between the normalized gradient value in the left hemisphere minus the gradient values in the right hemisphere.

Statistical Analyses. Statistical analysis was performed using R[124] (R version 4.1.0). Brain visualization was realized using Surf Ice[125].

Language Lateralization Identification – Using the same methodology as by Labache and colleagues[25], the 995 participants have been classified using agglomerative hierarchical clustering. Each participant was characterized according to their language network organization. Language network was described by 5 features: network- and hubs-level asymmetry during the language task, sum and asymmetry of strength, and homotopic inter-hemispheric connectivity value at rest. Hierarchical classification allowed for the identification of language lateralization for each individual. Briefly, hierarchical agglomerative clustering[126] was performed using Euclidean distance as metric and Ward's criterion as linkage criteria[127]. Each variable was standardized before classification. Number of clusters was set to 3 based on previous results[25]. The 3 clusters defined the language lateralization phenotype.

Using analysis of covariance, the broader relationship between language lateralization and the 5 features was assessed. Each of the 5 models was specified as follows: the features were the dependant variable, language lateralization phenotype was the independent variable, age, intracranial volume (FreeSurfer-derived), gender, and handedness as covariate, as well as the interaction handedness × language lateralization phenotype. Post-hoc analyses were conducted using Tukey's range test for multiple comparisons, or Student's t-test for binary ones.

Language Lateralization impact on gradient asymmetry – Analysis of covariance was used to assess the broader relationship between language lateralization and lateralization of large-scale cortical organization, modeled by gradient asymmetry. For each gradient and network, the model was specified as follows: gradient asymmetry for a given network and a given gradient was the dependant variable, language lateralization phenotype was the independent variable, age, intracranial volume (FreeSurfer-derived), gender, and handedness as covariate, as well as the interaction handedness × language lateralization phenotype. Bonferroni correction of significance thresholds was used to account for 7 independent tests of a given gradient. Post-hoc analyses were conducted using Tukey's range test for multiple comparisons, or Student's *t*-test for binary ones.

Heritability of Gradient Asymmetry and Language Lateralization Phenotype – Heritability is a statistic indicating to what extent the variation in a phenotypic trait is accounted for by the combined effects of genetic variations over the genome of a population. Heritability estimates range from 0 to 1. The heritability of gradient network asymmetry was estimated using SOLAR[67] (version: 9.0.0) through the R package *solarius*[128] (R package version: 0.3.2). Heritability covarying for age, sex, age^2, age × sex, age^2 × sex, handedness, and FreeSurfer-derived intracranial volume. Bonferroni correction of significance thresholds was used to account for 7 independent tests of heritability. Heritability of language lateralization phenotype (*i.e.* being typical or atypical) was also assessed using the same covariates.

Heritability estimates were conducted on 989 HCP participants, composed of 130 MZ twins (n = 260), 70 DZ twins (n = 140), non-twin siblings (n = 479), and unrelated singletons (n = 110).

Data availability

This study used publicly available data from the HCP (https://www.humanconnectome.org/). Data can be accessed via data use agreements. The language atlas is available here: https://github.com/loiclabache/SENSAAS_brainAtlas.

Code availability

The code used in the method section to process the data from the HCP and reproduced the results can be found here: https://github.com/loiclabache/Labache_2022_AO.

References

107. Oldfield, R. C. The assessment and analysis of handedness: the Edinburgh inventory. Neuropsychologia 9, 97–113 (1971).
108. Hervé, P.-Y., Crivello, F., Perchey, G., Mazoyer, B. & Tzourio-Mazoyer, N. Handedness and cerebral anatomical asymmetries in young adult males. Neuroimage 29, 1066–1079 (2006).
109. Papadatou-Pastou, M. et al. Human handedness: A meta-analysis. Psychol. Bull. 146, 481–524 (2020).
110. Coren, S. & Porac, C. Fifty centuries of right-handedness: the historical record. Science vol. 198 631–632 Preprint at https://doi.org/10.1126/science.335510 (1977).
111. Smith, S. M. et al. Resting-state fMRI in the Human Connectome Project. NeuroImage vol. 80 144–168 Preprint at https://doi.org/10.1016/j.neuroimage.2013.05.039 (2013).
112. Binder, J. R. et al. Mapping anterior temporal lobe language areas with fMRI: a multicenter normative study. Neuroimage 54, 1465–1475 (2011).
113. Glasser, M. F. et al. The minimal preprocessing pipelines for the Human Connectome Project. NeuroImage vol. 80 105–124 Preprint at https://doi.org/10.1016/j.neuroimage.2013.04.127 (2013).
114. Muschelli, J. Human 'Connectome' Project Interface [R package neurohcp version 0.9.0]. (2020).
115. Clayden, J. et al. RNifti: Fast R and C++ access to NIfTI images. (Github, 2021).
116. Van Essen, D. C., Glasser, M. F., Dierker, D. L., Harwell, J. & Coalson, T. Parcellations and hemispheric asymmetries of human cerebral cortex analyzed on surface-based atlases. Cereb. Cortex 22, 2241–2262 (2012).
117. Marcus, D. S. et al. Informatics and data mining tools and strategies for the human connectome project. Front. Neuroinform. 5, 4 (2011).
118. Zuo, X.-N., Xu, T. & Milham, M. P. Harnessing reliability for neuroscience research. Nat Hum Behav 3, 768–771 (2019).
119. Mesulam, M. M. From sensation to cognition. Brain 121 (Pt 6), 1013–1052 (1998).
120. Python Software Foundation. Python Language Reference. (2021).
121. Vos de Wael, R. et al. BrainSpace: a toolbox for the analysis of macroscale gradients in neuroimaging and connectomics datasets. Commun Biol 3, 103 (2020).
122. Coifman, R. R. et al. Geometric diffusions as a tool for harmonic analysis and structure definition of data: diffusion maps. Proc. Natl. Acad. Sci. U. S. A. 102, 7426–7431 (2005).
123. Lafon, S. & Lee, A. B. Diffusion maps and coarse-graining: A unified framework for dimensionality reduction, graph partitioning, and data set parameterization. IEEE Trans. Pattern Anal. Mach. Intell. 28, 1393–1403 (2006).
124. R Core Team. R: A language and environment for statistical computing. (R Foundation for Statistical Computing, 2021).
125. NITRC: Surf Ice: Tool/Resource Info. www.nitrc.org/projects/surfice/.
126. Sneath, P. H. A. & Sokal, R. R. Numerical Taxonomy: The Principles and Practice of Numerical Classification. (W H Freeman & Company, 1973).
127. Ward, J. H., Jr. Hierarchical grouping to optimize an objective function. J. Am. Stat. Assoc. 58, 236–244 (1963).
128. Ziyatdinov, A. et al. solarius: an R interface to SOLAR for variance component analysis in pedigrees. Bioinformatics 32, 1901–1902 (2016).

Acknowledgments

This work was supported by the National Institute of Mental Health (R01MH120080 and R01MH123245 to AJH) as well as by the following awards to BTTY: the Singapore National Research Foundation (NRF) Fellowship (Class of 2017), the NUS Yong Loo Lin School of Medicine (NUHSRO/2020/124/TMR/LOA), the Singapore National Medical Research Council (NMRC) LCG (OFLCG19May-0035), and the NMRC STaR (STaR20nov-0003). Any opinions, findings and conclusions or recommendations expressed in this material are those of the authors and do not reflect the views of the Singapore NRF or the Singapore NMRC. Data were in part provided by the Human Connectome Project, WU-Minn Consortium (Principal Investigators: David Van Essen and Kamil Ugurbil; 1U54MH091657) funded by the 16 NIH Institutes and Centers that support the NIH Blueprint for Neuroscience Research; and by the McDonnell Center for Systems Neuroscience at Washington University.

Competing interests

The authors declare no competing interests.

Supplementary Materials

Atypical language network lateralization is reflected throughout the macroscale functional organization of cortex

Loïc Labache[a,*], Tian Ge[b, c, d], B.T. Thomas Yeo[e, f, g, h, i], Avram J. Holmes[a, j, k]

Demographic characterization according to language lateralization phenotype

Pearson's chi-squared test showed a significant effect of language lateralization phenotype on handedness (χ^2=32.07, p<1.10^{-4}). There were significantly more left-handers in the atypical group than in the strong typical (χ^2=41.81, p<1.10^{-4}), and than in the mild typical ones (χ^2=23.83, p<1.10^{-4}). No differences in proportion between mild and strong typical (χ^2=3.50, p=0.061).

Pearson's chi-squared test showed a significant effect of language lateralization phenotype on sex (χ^2=71.44, p<1.10^{-4}). There were significantly more females in the mild atypical group than in the atypical (χ^2= 9.71, p=0.002), and than in the strong typical group (χ^2=71.17, p<1.10^{-3}). No differences in proportion between atypical and strong typical (χ^2=2.89, p=0.089).

Analysis of variance showed a significant effect of language lateralization phenotype on age (p<1.10^{-3}). Mild typical individuals (μ=29.52 years, 95% confidence interval (CI)=±0.34 years) were older than atypical (μ=27.96 years, CI=±0.79 years, p=0.0012) and strong typical (μ=28.08 years, CI=±0.33 years, p<1.10^{-4}). Atypical and strong typical individuals were the same age (p=0.96).

Analysis of variance showed a significant effect of language lateralization phenotype on educational level (p=0.033). Tukey's HSD post-hoc test, which is conservative, reported no significant post-hocs tests. Strong typical individuals (μ=15.11 years, CI=±0.16 years) were not significantly different from mild typical (μ=14.86 years, CI=±0.17 years, $p_{corrected}$=0.077, $p_{uncorrected}$=0.03), or atypicals (μ=14.70 years, CI=±0.39 years, $p_{corrected}$=0.12, $p_{uncorrected}$=0.048). Atypical individuals were not significantly different from mild typical ones ($p_{corrected}$=0.72, $p_{uncorrected}$=0.44). That means that even if each pair of phenotypes were not significantly different from each other, there may exist a contrast (*i.e.* a combination or contrast of phenotypes) that is significant.

[a] Department of Psychology, Yale University, New Haven, US-CT 06520. [b] Psychiatric and Neurodevelopmental Genetics Unit, Center for Genomic Medicine, Massachusetts General Hospital, Boston, US-MA 02114. [c] Center for Precision Psychiatry, Department of Psychiatry, Massachusetts General Hospital, Boston, US-MA 02114. [d] Stanley Center for Psychiatric Research, Broad Institute, Cambridge, US-MA 02142. [e] Department of Electrical and Computer Engineering, Centre for Sleep and Cognition, National University of Singapore, Singapore, SG 119077. [f] Department of Electrical and Computer Engineering, Centre for Translational Magnetic Resonance Research, National University of Singapore, Singapore, SG 119077. [g] N.1 Institute for Health, National University of Singapore, Singapore, SG 119077. [h] Martinos Center for Biomedical Imaging, Massachusetts General Hospital, Charlestown, US-MA 02129. [i] National University of Singapore Graduate School for Integrative Sciences and Engineering, National University of Singapore, Singapore, SG 119077. [j] Department of Psychiatry, Yale University, New Haven, US-CT 06520. [k] Wu Tsai Institute, Yale University, New Haven, US-CT 06520. *e-mail: loic.labache@yale.edu

Language lateralization phenotype	Demographics variables	
Atypical	Sex	*n* = 41 female
	Handedness	*n* = 26 left-handers
	Average age (± 95% CI)	27.96 ± 0.79 years
	Average educational level (± 95% CI)	14.70 ± 0.39 years
Mild typical	Sex	*n* = 294 female
	Handedness	*n* = 48 left-handers
	Average age (± 95% CI)	29.52 ± 0.34 years
	Average educational level (± 95% CI)	15.11 ± 0.16 years
Strong typical	Sex	*n* = 192 female
	Handedness	*n* = 36 left-handers
	Average age	28.08 ± 0.33 years
	Average educational level (± 95% CI)	14.86 ± 0.17 years

Supplementary Table 1. | HCP demographics according to language lateralization phenotype.

Details of the ANCOVA results for the 5 features used to classify individuals

Effect	*p*-value	Levels	Least Squares Mean/Regression slope	95% Confidence Interval
Age	0.06	-	-	-
Gender	0.01	female	0.41	±0.11
		male	0.58	±0.14
Intracranial volume	0.77	-	-	-
Language lateralization phenotype	$<10^{-4}$	atypical	-0.96	±0.18
		mild-typical	0.70	±0.12
		strong-typical	1.74	±0.14
Handedness	$<10^{-3}$	left-handers	0.34	±0.15
		right-handers	0.65	±0.08
Language lateralization phenotype × Handedness	0.14	-	-	-

Supplementary Table 2. | ANCOVA's results of the asymmetry during the language task at the network level.

Effect	*p*-value	Levels	Least Squares Mean/Regression slope	95% Confidence Interval
Age	0.15	-	-	-
Gender	0.21	-	-	-
Intracranial volume	0.63	-	-	-
Language lateralization phenotype	$<10^{-4}$	atypical	-1.16	±0.26
		mild-typical	1.17	±0.17
		strong-typical	2.64	±0.19
Handedness	$<10^{-3}$	left-handers	0.66	±0.22
		right-handers	1.11	±0.11
Language lateralization phenotype × Handedness	0.33	-	-	-

Supplementary Table 3. | ANCOVA's results of the asymmetry during the language task at the epicenters level.

Effect	*p*-value	Levels	Least Squares Mean/Regression slope	95% Confidence Interval
Age	0.82	-	-	-
Gender	0.76	-	-	-
Intracranial volume	0.99	-	-	-
Language lateralization phenotype	$<10^{-4}$	atypical	9.10^{-3}	±0.18
		mild-typical	0.85	±0.12
		strong-typical	1.02	±0.13
Handedness	0.27	-	-	-
Language lateralization phenotype × Handedness	0.13	-	-	-

Supplementary Table 4. | ANCOVA's results of the strength asymmetry at rest.

Effect	*p*-value	Levels	Least Squares Mean/Regression slope	95% Confidence Interval
Age	$<10^{-4}$	-	-0.10	±0.04
Gender	$<10^{-4}$	female	10.74	±0.31
		male	11.67	±0.31
Intracranial volume	0.004	-	2.10^{-6}	$\pm1.10^{-6}$
Language lateralization phenotype	$<10^{-4}$	atypical	12.06	±0.53
		mild-typical	9.4	±0.35
		strong-typical	12.16	±0.39
Handedness	0.28	-	-	-
Language lateralization phenotype × Handedness	0.30	-	-	-

Supplementary Table 5. | ANCOVA's results of the strength sum at rest.

Effect	*p*-value	Levels	Least Squares Mean/Regression slope	95% Confidence Interval
Age	$<10^{-4}$	-	-0.01	$\pm2.10^{-3}$
Gender	0.01	female	0.56	±0.01
		male	0.58	±0.02
Intracranial volume	0.04	-	5.10^{-8}	$\pm5.10^{-8}$
Language lateralization phenotype	$<10^{-4}$	atypical	0.61	±0.03
		mild-typical	0.49	±0.02
		strong-typical	0.61	±0.02
Handedness	0.75	-	-	-
Language lateralization phenotype × Handedness	0.13	-	-	-

Supplementary Table 6. | ANCOVA's results of the homotopic inter-hemispheric connectivity value at rest.

Full description of ANCOVAs performed on gradient asymmetries

	Default	Control	Limbic	Sal/VentAttn	DorsAttn	Som/Motor	Visual
R^2_{model} (%)	5.65	5.39	1.47	3.09	2.33	0.04	5.39
p-value$_{model}$	$<1.10^{-4}$	$<1.10^{-4}$	0.023	$<1.10^{-4}$	$<1.10^{-3}$	0.75	$<1.10^{-4}$
Age	*p*=0.58	*p*=0.68	*p*=0.96	*p*=0.22	*p*=0.71	*p*=0.11	*p*=0.99
ITV	*p*=0.61	*p*=0.004 $\beta=3.10^{-6}$ $\pm 2.10^{-6}$	*p*=0.49	*p*=0.88	*p*=0.83	*p*=0.35	*p*=0.79
Gender	*p*=0.02	*p*=0.26	*p*=0.24	*p*=0.16	*p*=0.13	*p*=0.70	*p*=0.06
MP	*p*=0.002 RH: 1.04 ±0.58 LH: -0.75 ±0.95	*p*=0.19	*p*=0.62	*p*=0.36	*p*=0.02	*p*=0.91	*p*=0.02
MP x LLP	*p*=0.006 $LH_{atypical}$: -3.3 ±1.65 $RH_{atypical}$: 0.05 ±1.112 $LH_{typical}$: 1.79 ±0.92 $RH_{typical}$: 2.02 ±0.29	*p*=0.78	*p*=0.08	*p*=0.61	*p*=0.04	*p*=0.76	*p*=0.25

Supplementary Table 7. | ANCOVA's results of the frist gradient asymmetries values. ITV corresponds to the Intracranial Volume (FreeSurfer-derived), MP to the handedness, LLP to Language Lateralization Phenotype, RH to Right-Handers, LH to Left-Handers. The least square mean plus or minus the 95% confidence interval is reported when the main effect is significant.

	Default	Control	Limbic	Sal/VentAttn	DorsAttn	Som/Motor	Visual
R^2_{model} (%)	1.72	2.5	0.58	1.33	0.78	1.12	5.39
p-value$_{model}$	0.009	0.0003	0.45	0.04	0.26	0.083	$<1.10^{-4}$
Age	*p*=0.99	*p*=0.37	*p*=0.42	*p*=0.85	*p*=0.63	*p*=023	*p*=0.27
ITV	*p*=0.63	*p*=0.01	*p*=0.42	*p*=0.79	*p*=0.37	*p*=0.31	*p*=0.09
Gender	*p*=0.86	*p*=0.58	*p*=0.41	*p*=0.74	*p*=0.60	*p*=0.53	*p*=0.47
MP	*p*=0.01	*p*=0.27	*p*=0.97	*p*=0.02	*p*=0.02	*p*=0.03	*p*=0.26
MP x LLP	*p*=0.02	*p*=0.94	*p*=0.49	*p*=0.08	*p*=0.50	*p*=0.32	*p*=0.07

Supplementary Table 8. | ANCOVA's results of the second gradient asymmetries values. ITV corresponds to the Intracranial Volume (FreeSurfer-derived), MP to the handedness, LLP to Language Lateralization Phenotype, RH to Right-Handers, LH to Left-Handers. The least square mean plus or minus the 95% confidence interval is reported when the main effect is significant.

	Default	Control	Limbic	Sal/VentAttn	DorsAttn	Som/Motor	Visual
R^2_{model} (%)	17.23	12.94	3.60	5.86	1.76	1.70	1.65
p-value$_{model}$	$<1.10^{-4}$	$<1.10^{-4}$	$<1.10^{-4}$	$<1.10^{-4}$	0.007	0.01	0.01
Age	*p*=0.17	*p*=0.11	*p*=0.64	*p*=0.18	*p*=0.46	*p*=0.03	*p*=0.01
ITV	*p*=0.58	*p*=0.19	*p*=0.63	*p*=0.08	*p*=0.23	*p*=0.32	*p*=0.48
Gender	*p*=0.02	*p*=0.003 ♀: 4.85 ±1.23 ♂: 2.89 ±1.22	*p*=0.29	*p*=0.05	*p*=0.32	*p*=0.35	*p*=0.91
MP	$p<1.10^{-4}$ RH: 1.79 ±0.89 LH: 6.06 ±1.44	*p*=0.005 RH: 2.37 ±1.09 LH: 5.37 ±1.77	*p*=0.10	*p*=0.06	*p*=0.08	*p*=0.47	*p*=0.07
MP x LLP	*p*=0.011	*p*=0.59	*p*=0.46	*p*=0.54	*p*=0.04	*p*=0.29	*p*=0.59

Supplementary Table 9. | ANCOVA's results of the third gradient asymmetries values. ITV corresponds to the Intracranial Volume (FreeSurfer-derived), MP to the handedness, LLP to Language Lateralization Phenotype, RH to Right-Handers, LH to Left-Handers. The least square mean plus or minus the 95% confidence interval is reported when the main effect is significant.

Network	Gradient number	Typical (μ ±CI)	Atypical (μ ±CI)	*p-value*
Default	1	**1.91 ±0.48**	**-1.62 ±1.00**	**$<1.10^{-4}$**
	2	**-0.54 ±0.26**	**-1.58 ±0.53**	**$<1.10^{-3}$**
	3	**-1.20 ±0.73**	**9.05 ±1.52**	**$<1.10^{-4}$**
Control	1	**-6.21 ±0.59**	**-9.21 ±1.21**	**$<1.10^{-4}$**
	2	**-2.93 ±0.36**	**-4.26 ±0.74**	**0.002**
	3	**-0.77 ±0.90**	**8.51 ±1.87**	**$<1.10^{-4}$**
Limbic	1	2.88 ±0.75	1.76 ±1.55	0.20
	2	-0.63 ±0.48	-1.28 ±0.99	0.25
	3	**-2.53 ±0.71**	**1.57 ±1.47**	**$<1.10^{-4}$**
Sal/VentrAttn	1	**1.11 ±0.51**	**-1.65 ±1.05**	**$<1.10^{-4}$**
	2	**1.26 ±0.44**	**-0.17 ±0.92**	**0.006**
	3	**-4.26 ±0.63**	**-1.25 ±1.31**	**$<1.10^{-4}$**
DorsAttn	1	**4.09 ±0.54**	**1.56 ±1.11**	**$<1.10^{-4}$**
	2	0.88 ±0.53	0.52 ±1.10	0.56
	3	-0.61 ±0.67	1.50 ±1.39	0.008
Som/Motor	1	0.01 ±0.24	-0.02 ±0.50	0.91
	2	-2.52 ±0.41	-1.77 ±0.85	0.12
	3	0.34 ±0.34	0.84 ±0.71	0.22
Visual	1	**1.60 ±0.26**	**0.67 ±0.53**	**0.002**
	2	-0.24 ±0.29	0.29 ±0.61	0.12
	3	0.53 ±0.28	1.12 ±0.58	0.07

Supplementary Table 10. | Post-hoc results of the language lateralization main effect. Bold cells are cells with a significant corrected effect (Bonferroni correction for network number, p<0.007). μ corresponds to the least square mean value of the model. CI corresponds to the 95% Confidence Interval of μ.

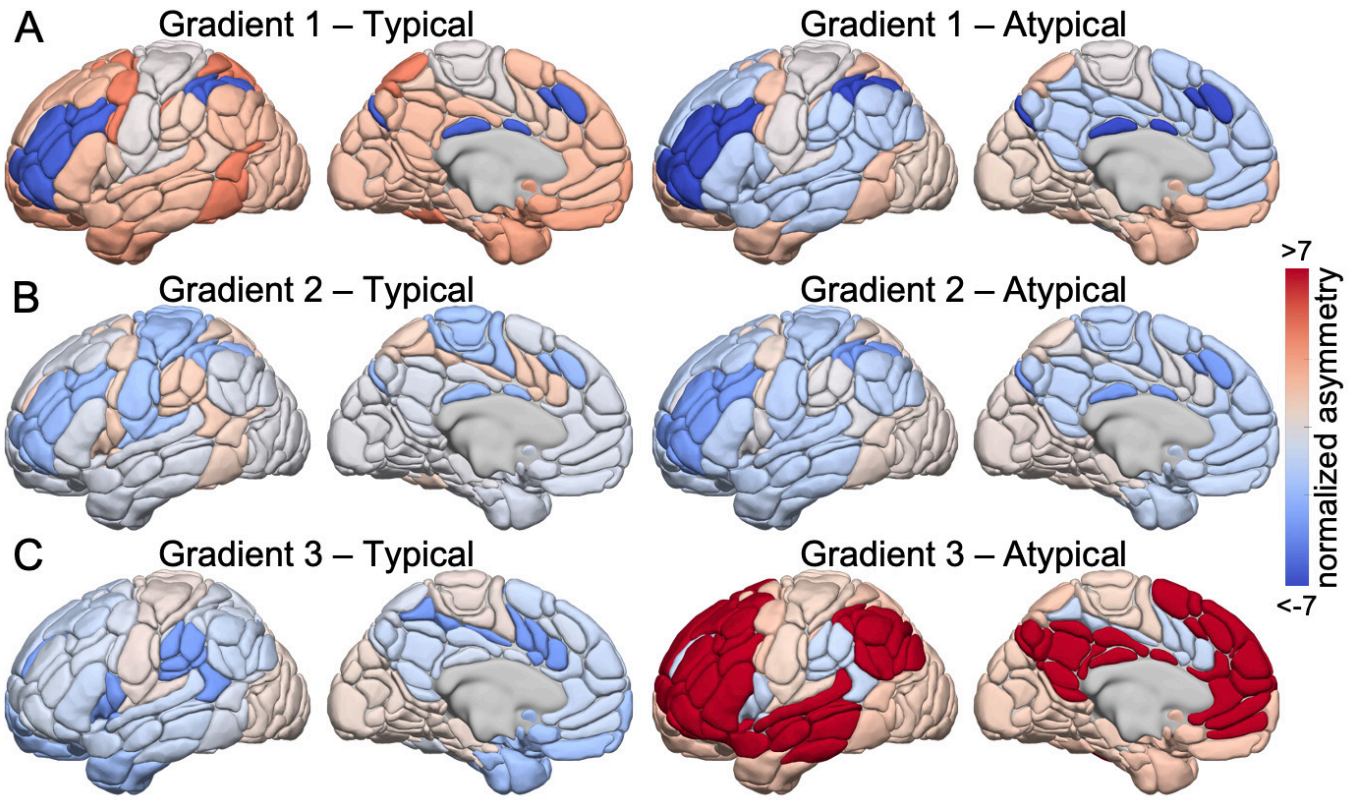

Supplementary Figure 1. | Average gradients asymmetries values of functional connectivity across the cortical sheet (left minus right normalized gradient values). Asymmetries for typical individual (left hemisphere dominant for language) on the left, atypical individuals (right dominant) on the right. **(A)** Asymmetries values for the principal gradient of connectivity that transitions from the unimodal to the association cortex. **(B)** Asymmetries values for the second gradient that primarily differentiates the somato/motor and auditory cortex from the visual system. **(C)** Asymmetries values for the third gradient that reflects a network architecture contrasting frontoparietal from default and somato/motor systems. Warmer colors (solid red) indicate leftward asymmetries, colder colors (solid blue) reflects rightward asymmetries.

Heritability of gradients asymmetry at the networks level

	Network	Heritability (h^2)	Standard Error	*p-value*
Gradient 1	**Default ***	**0.22**	**0.06**	**$<1.10^{-4}$**
	Control *	**0.19**	**0.06**	**$<1.10^{-3}$**
	Limbic	0.09	0.07	0.089
	Sal/VentAttn *	**0.25**	**0.06**	**$<1.10^{-4}$**
	DorsAttn *	**0.2**	**0.06**	**$<1.10^{-3}$**
	Som/Motor	0.08	0.05	0.05
	Visual	0.08	0.06	0.07
Gradient 2	**Default ***	**0.16**	**0.06**	**0.003**
	Control *	**0.14**	**0.06**	**0.01**
	Limbic	0.03	0.05	0.28
	Sal/VentAttn	0.08	0.06	0.08
	DorsAttn	0.02	0.06	0.35
	Som/Motor	0.06	0.06	0.14
	Visual	0.02	0.05	0.32
Gradient 3	**Default ***	**0.28**	**0.06**	**$<1.10^{-4}$**
	Control *	**0.28**	**0.06**	**$<1.10^{-4}$**
	Limbic *	**0.16**	**0.06**	**0.003**
	Sal/VentAttn *	**0.22**	**0.06**	**$<1.10^{-4}$**
	DorsAttn *	**0.18**	**0.06**	**$<1.10^{-3}$**
	Som/Motor	0.00	0.00	0.50
	Visual	0.09	0.06	0.06

Supplementary Table 11. | Heritability of individualized gradient values are greater in heteromodal (h^2: μ=18.5%, SD=7.7%) relative to unimodal (h^2: μ=5.5%, SD=3.8%) networks (p=0.001). Heritability of individual gradient value was estimated across 7 canonical functional networks using SOLAR67. Raws in bold are those remaining significant effects after Bonferroni correction for network number (p≤0.007).

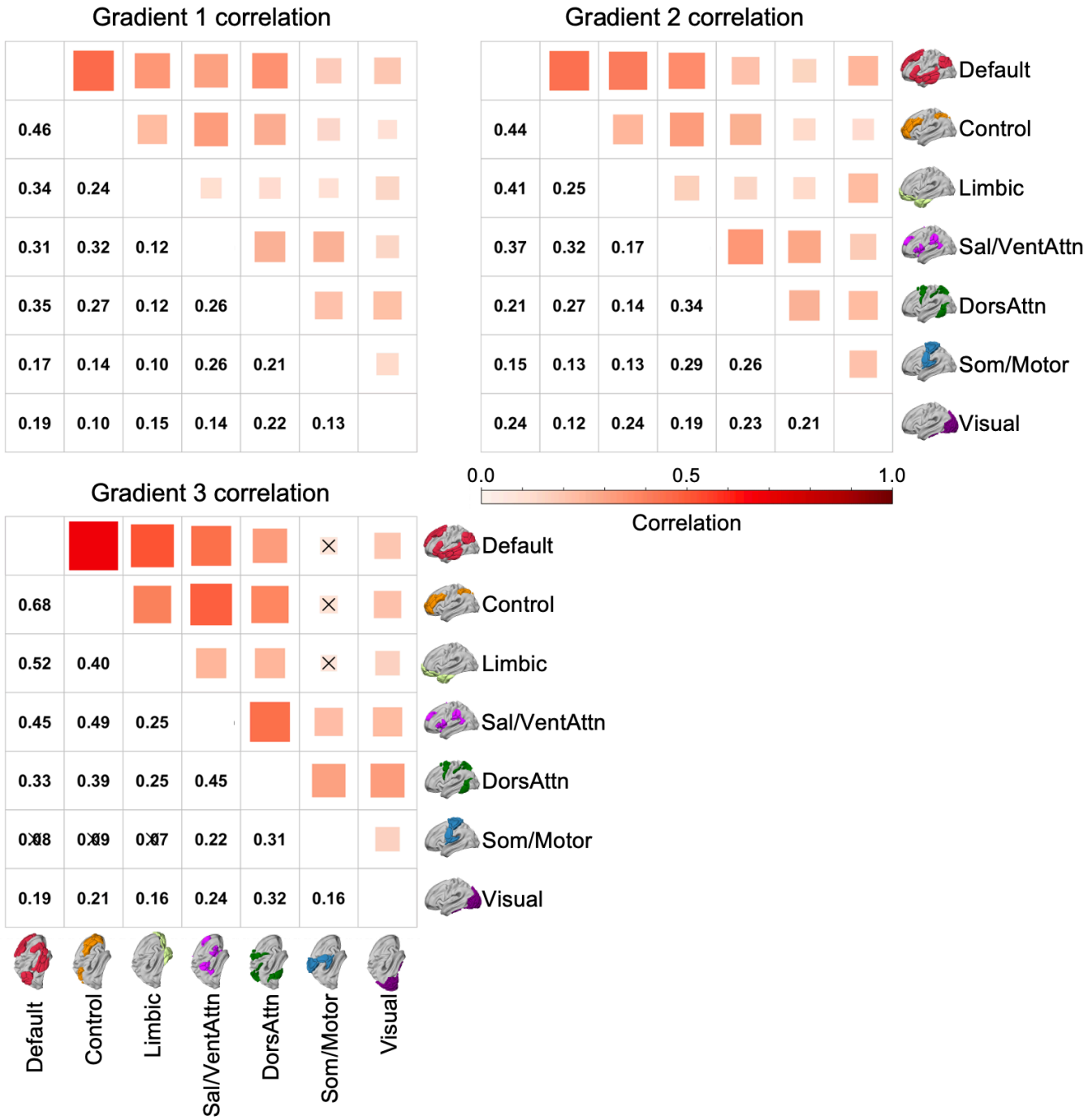

Supplementary Figure 2. | Asymmetry gradient correlations for each network across participants. The upper part of the matrix showed the strength of the correlation: The size of the squares (dark red) reflect the strength of the associated correlation. The lower part of the matrix shows the correlation values. Each correlation coefficient was significant (Bonferroni corrected for 21 tests, $p<(0.05/21)=0.0024$), except as indicated by a cross.